SOLUTION CONFORMATION OF ENOPEPTIN A, A DEPSIPEPTIDE ANTIBIOTIC, USING 2D NMR AND RESTRAINED MOLECULAR DYNAMICS STUDIES

JENN-JONG YOUNG, LIARNG-JYUR JUNG, WEN-TSSANN LIU, SU-NENG HO, LI-REN CHANG, YI-CHUN TSAI[a], RAJAGOPALAN BHASKARAN[b,†] and CHIN YU[b,*]

Institute of Preventive Medicine, National Defence Medical Center, Taipei, Taiwan, R.O.C.
[a]National Center for High Performance Computing, Hsinchu, Taiwan, R.O.C.
[b]Department of Chemistry, National Tsing Hua University, Hsinchu, Taiwan, R.O.C.

(Received for publication January 17, 1994)

Studies on the solution conformation of the cyclic depsipeptide antibiotic enopeptin A have been carried out using 2D NMR and molecular modelling techniques. The proton resonances of the antibiotic in DMSO-d_6 have been assigned by the use of TOCSY and ROESY experiments. The interproton distance information obtained from the ROESY experiments have been used as the basis for elucidating the probable structures in solution. The restrained molecular dynamics technique was applied to calculate the structures in solution, and six resultant structures with fewer distance constraint violations were obtained that satisfy the experimental restraints very well. The conformation of the cyclic moiety of the molecule is well defined whereas the aliphatic chain segment is disordered.

Enopeptin A, a novel depsipeptide antibiotic exhibits antibacteriophage activity in the assay system using actinophage B1 and *Streptomyces griseus*.[1,2] It inhibits the plaque formation of bacteriophage B. It also shows anti-microbial activity against Gram-positive bacteria including a methicillin-resistant *Staphylococcus aureus* and Gram-negative mutants that are defective in the cell membrane. However the antibiotic was not inhibitory to fungi. Enopeptin A consists of the amino acids Ala, Pro, Phe, Ser and two unusual amino acids, *N*-methylalanine (MeAla) and 4-methylproline (MePro).[2] In addition, it has a long tail segment consisting of 1,3,5,7,9-decapentaene-1,10-dicarboxylic acid [$CO(CH=CH)_5CO$] and 2-amino-3-hydroxy-cyclopent-2-enone (AHCPE) moities. The amino acids, other than Phe, form the cyclic portion of the molecule in which MePro lies between Ser and Ala, MeAla between Ala and Pro. The cyclic peptide segment is linked to the linear tail segment by the Phe residue. The chemical structure of enopeptin A is given in Fig. 1. The cyclic moiety is expected to play a leading role in the molecular activity because of the narrow cavity it possesses and because of the hydrophobic nature of the residue side chains. Complete understanding of the activity may develop from the finer structural details of the molecule with knowledge of its three-dimensional structure. Further conformational analysis of the molecule will yield information about the positioning and hence role of specific functional groups in the mode of action. To date the three-dimensional structure of the molecule is not available either from X-ray diffraction or NMR. Although two-dimensional nuclear magnetic resonance (2D NMR) studies in $CDCl_3$ solution have been carried out on the molecule,[2] the complete 3D structure in solution has not been attempted so far. Recently conformational analyses of antibiotics[3~8] and cyclic peptides[9~12] have been possible due to the advancement of 2D NMR spectroscopy. In order to understand in detail the structural aspects suitable for

† Permanent Address: Department of Physics, Bharathidasan University, Tiruchirapalli-620 024, India.

Fig. 1. The molecular formula of enopeptin A.

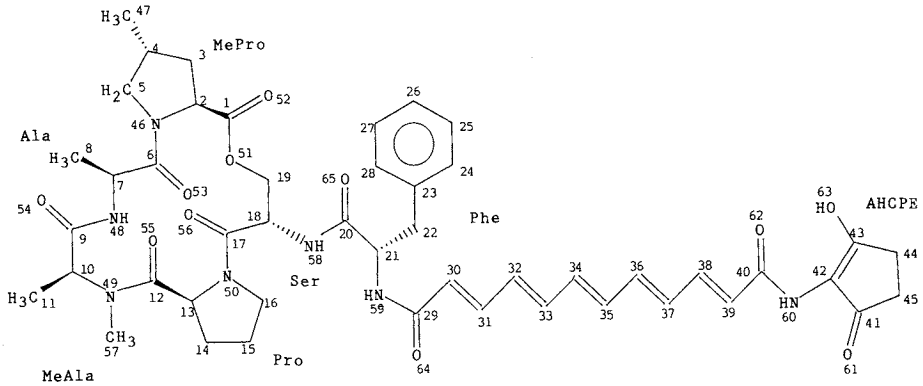

molecular activity, we carried out investigations to determine the structures in solution. We report here the determination of the 3D structure of enopeptin A in DMSO-d_6 solution by the combined use of 2D NMR and restrained molecular dynamics (RMD) techniques.[13] The structures calculated using the above methods revealed a well ordered conformation for the cyclic moiety of the molecule but an ill-defined one for the linear aliphatic chain segment.

Materials and Methods

Fermentation

The producing organism designated *Streptomyces* sp. ZZ1-10 was isolated from Kao-Shung county, Taiwan. The procedures for the fermentation and isolation were slightly modified from the earlier work[1] as follows. One loopful of a culture of *Streptomyces* sp. ZZ1-10 from an ISP M4 agar slant was inoculated into a conical flask (500 ml) containing 100 ml Tryptic Soy Broth medium (100 ml, TSB, Difco), and incubated on a rotary shaker (200 rpm) at 27°C for two days. Then the primary seed culture was inoculated into a fermentor (7 liters) containing seed medium (5 liters) with the following composition: yeast extract 0.5%, cotton seed flour (Sigma) 0.5%, $MgSO_4 \cdot H_2O$ 0.1%, K_2HPO_4 0.1%. The pH was adjusted to 7.1 before sterlization. After cultivation under agitation of 200 rpm and aeration of 20 liters/minute at 27°C for 24 hours, a 5% inoculum of the second seed culture was transfered into a fermentor (Chemap-CF150) containing production medium (100 liters) consisting of dextrose 1%, NaCl 0.2%, soy bean meal 1%, K_2HPO_4 0.2%, $MnSO_4 \cdot H_2O$ 0.04%, $ZnSO_4 \cdot 7H_2O$ 0.044%, ferritartrate 0.005%. The fermentation was carried out under same conditions for five days. The antibiotic production was monitored by a paper-disc assay using *Staphylococcus aureus* ATCC 6538p as test organism.

Isolation

The culture supernatant, which was separated from fermentation broth by centrifugation, was extracted with EtOAc, and the organic layer was concentrated to a small volume under reduced pressure. Then the crude extract was adsorbed onto silica gel (80 g), evaporated to dryness and placed on a silica gel chromatography column (70~230 mesh, Merck) that was eluted stepwise with CH_2Cl_2-MeOH (100:1 to 15:1). The active fractions were combined, concentrated and applied to a second silica gel column (230~400 mesh, Merck) using CH_2Cl_2-MeOH (20:1) as the mobile phase. After column chromatography, enopeptin A was further purified by preparative TLC (Kieselgel $60F_{254}$) developed with $CHCl_3$-MeOH (15:1, Rf 0.53). This gave 22.0 mg of pure enopeptin A as a yellowish-orange crystalline powder by precipitation from $CHCl_3$ by the addition of *n*-hexane.

NMR Experiments

The NMR sample of enopeptin A was prepared at a concentration of approximately 20 mM by

dissolving the antibiotic in deuterated dimethyl sulfoxide solution (500 μl, Aldrich). Sodium 4,4-dimethyl-4-silapentane-1-sulfonate was used as an internal standard. The NMR tube (5 mm) was degassed and sealed. All NMR spectra were recorded on a 300 MHz spectrometer (Varian Unity-300), and the data were processed using VNMR software. The COSY experiment was carried out in the absolute value mode.[14] Phase sensitive TOCSY[15,16] and ROESY[17,18] spectra were acquired (mixing periods 50, 100, 150, 200, 250, 300, 400 and 500 ms) with 2048 complex data points in t_2 and 512 points in t_1 with a spectral width of 3302.8 Hz. All experiments were performed with quadrature detection in the phase sensitive mode using 2D hypercomplex (States-Haberkorn) method. The data were apodized using a Guassian function in both dimensions. Prior to Fourier transformation the time domain data were zero filled once.

NMR Parameters

The distance extrapolation method was used to compute interproton distances.[19,20] According to this method, the interproton distances of all proton pairs were derived from a comparison with a standard NOE corresponding to geminal proton pairs in each mixing period, respectively. Least-squares lines were fitted through all distances computed for the mixing periods and they were extrapolated to zero mixing time. The respective intercept values refer to the interproton distances between the proton pairs. The vicinal proton coupling constants indicate dihedral angle dependence of the Karplus type and hence yield information on the backbone conformation of the molecule.[21] Vicinal $^3J_{HN\alpha}$ and the other proton coupling constants were measured from the splittings of their amide resonances in the 1D spectrum.

Computational Methods

In order to determine the conformation of enopeptin A in solution, RMD technique was attempted. All computations were performed on a Silicon Graphics workstation 4D/35G. The RMD calculations were carried out using the software CHARMm.[22] The molecular graphics software QUANTA (Molecular Simulations Inc.) was used to generate, display, analyse and plot the molecular structures. An empirical energy function that includes terms for bond lengths, bond angles, dihedral angles and functions for van der Waals and electrostatic interactions was used in the calculation of molecular dynamics simulation. All possible non-bonded interactions within a cut-off radius of 14 Å were included. The presence of solvent molecules was effected by the inclusion of a distance-dependent dielectric constant into the computations. The NOE distance information was incorporated by including a distance restraint function which involves the calculated and target interproton distances, the Boltzmann constant and the temperature of the system. First, an initial structure of the molecule was constructed by means of the small molecular model building program of QUANTA and was used as the starting structure for RMD simulation.

Results

Assignment of Proton Signals

The ^{1}H NMR resonances were assigned by combining the *J* connectivity information from the COSY and TOCSY spectra and the through space connectivities from the ROESY spectra.[23] Chemical shifts of the proton resonances, multiplicities and coupling constants are summarized in Table 1. The coupling between one of the H_β of Phe with its H_α was so small that its coupling constant could not be measured clearly. To start with the assignment, the spin systems of Ala, Ser and Phe were unambiguously assigned from the TOCSY spectrum based on the following, respectively: 1) the H_α connectivity to the methyl resonance for Ala; 2) the lower field chemical shift for H_β of Ser; and 3) the geminal H_β coupling pattern of the AMX spin system of Phe. The aromatic spin systems of Phe could be uniquely assigned using the intraresidue ROE connectivities between the ring and H_β observed in the ROESY spectra. Protons of the other residues and the olefinic part of the molecule were easily traced from a combination of TOCSY and ROESY spectra with the use of the through bond and through space connectivities, respectively. Fig. 2

Table 1. Proton chemical shifts, multiplicities and coupling constants for enopeptin A in DMSO-d_6.

Proton[a]		Chemical shift (multiplicity) (ppm)	Coupling constant (Hz)	Proton[a]		Chemical shift (multiplicity) (ppm)	Coupling constant (Hz)
MePro	H_α (2)	4.39 (d)	8.4		H_γ (15)	1.92 (m)	
	H_β (3)	2.00, 1.88 (m)			H_δ (16)	3.54, 3.40 (m)	
	H_γ (4)	2.4 (m)		Ser	H_α (18)	4.46 (t)	9.6
	H_δ (5)	3.39 (m), 3.04 (d)	11.1		H_β (19)	4.90 (d), 3.60 (t)	6.0, 9.6
	CH_3 (4)	0.97 (d)	6.9		NH	8.94 (d)	9.6
Ala	H_α (7)	4.86 (m)		Phe	H_α (21)	4.59 (dd)	6.3, 6.6
	H_β (8)	1.21 (d)	7.2		H_β (22)	3.00 (d)	13.2
	NH	8.39 (d)	9.3			2.75 (dd)	6.3, 13.2
MeAla	H_α (10)	4.72 (q)	6.6		NH	7.51 (d)	6.6
	H_β (11)	1.42 (d)	6.6	AHCPE	CH(44, 45)	2.49 (s)	
	NCH_3	2.70 (s)			NH	10.05 (br s)	
Pro	H_α (13)	5.11 (d)	6.9		OH	13.91 (br s)	
	H_β (14)	2.50 (m)					

[a] The atom numbers corresponding to the carbon positions shown in Fig. 1 are given within the parenthesis.

Fig. 2. The TOCSY spectrum of enopeptin A in DMSO-d_6 showing some of the proton connectivities.

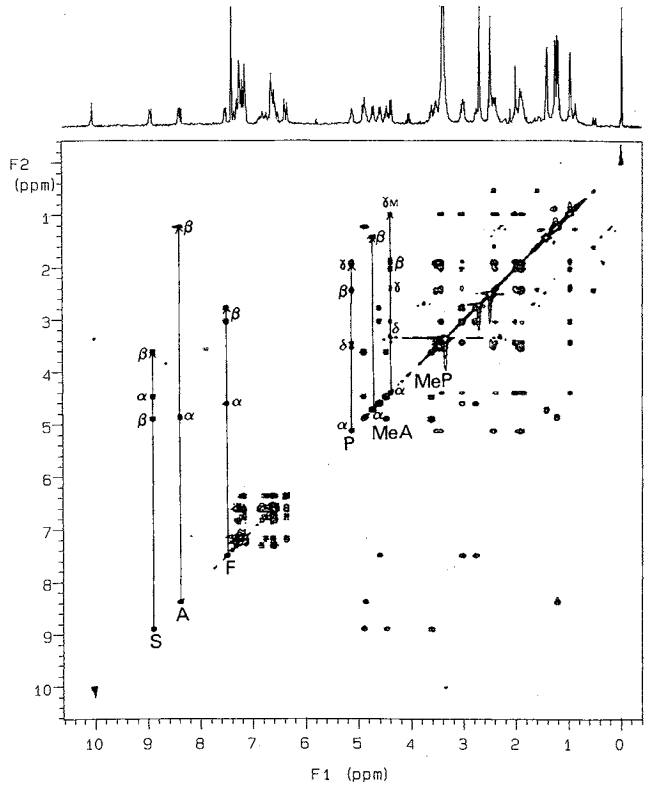

shows the full TOCSY spectrum of enopeptin A used for the assignment in which some diagonal peaks of specific protons are marked.

NMR Constraints

As the correlation time for this medium-sized molecule makes the cross relaxation rate nearly zero,

the NOESY spectra recorded at first were found to contain only a few weak cross peaks. This made us collect the ROESY data, as the rotating-frame cross relaxation experiments are expected to yield better results. As the ROESY intensity of the cross peaks are dependent on the offset from the rf carrier, the usual correction for the offset dependence has been incorporated.[9] For the computation of interproton distances, the average value of the volume integrals relative to the clearly resolved geminal proton pair ($H_\beta/H_{\beta'}$) of Phe was used as reference, for which an interproton distance of 1.8 Å was used as the standard. For the remaining other ROESY cross peaks the averages of the respective reference volumes, found on each side of the diagonal of the relevant ROESY spectra, were used for the distance computation. Least-squares lines were fitted for all proton pairs whose ROESY cross peaks were integrable, showing the relationship of the distances with the mixing periods. These lines were extrapolated to the ordinate to yield the distances between the respective protons (Fig. 3). Table 2 lists interproton distances derived from 29 strong ROESY cross peaks by the distance extrapolation method. Because of rotation of methyl groups, flipping of aromatic rings and inability to make stereo-specific assignments, pseudoatom correction factors were applied.[24] The maximum possible error due to introduction of pseudoatoms was incorporated with the constraints by additional correction terms. The upper bounds for the distance constraints were fixed by addition of 0.2 Å to the actual distances, due to experimental error. Thus a set of distance constraints (consisting of one trans-annular and nine sequential values) was derived, which formed the basis of the structure determination from the RMD simulation.

Fig. 3. Time dependence of some rotating frame NOEs in enopeptin A measured from the ROESY spectra for different mixing periods.

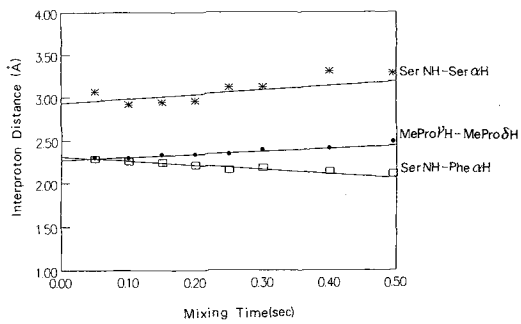

The extrapolation of the least squares fitted lines to zero mixing period yields interproton distances.

Calculation of Solution Structures

As the energy minimization explores only the conformation of a single static structure, we applied the following RMD protocol on the initial structure that can overcome energy barriers of magnitude kT and carry the system into regions of other conformational energy minima, depending on the kinetic

Table 2. Interproton distances computed from rotating frame NOEs for enopeptin A.

Proton pair		Interproton distances (Å)	Proton pair		Interproton distances (Å)
Atom 1	Atom 2		Atom 1	Atom 2	
Ser NH	Phe H_α	2.30	Phe H_α	Phe H_β	2.74
Ser H_β	Ser NH	2.65	MePro H_δ	MePro H_γ	2.27
Ala NH	Ala H_α	2.66	Pro H_δ	Pro H_γ	2.05
Ala NH	MeAla H_α	2.87	MeAla NCH_3	MeAla H_β	2.44
Ala NH	Ser H_α	3.27	Pro H_β	Pro H_γ	2.01
Ala NH	MeAla NCH_3	2.57	MePro H_γ	MePro CH_3	2.30
Ala NH	Ala H_β	2.57	Pro H_γ	MeAla H_β	2.95
Pro H_α	Ser H_α	3.22	MePro H_β	MePro CH_3	2.70
Ala H_α	MePro H_α	3.65	Ser NH	Ser H_α	2.81
Ala H_α	Ala H_β	2.92	MePro H_α	MePro H_β	2.56
MeAla H_α	MeAla H_β	2.34			

energy of the system and the time allowed to search the conformational space. At first, unconstrained energy minimization for 100 steps of steepest descent followed by 500 steps of conjugate gradient method was carried out on the molecule to remove the strains caused by defining the inter-chain bonds. The molecule was then gradually heated from 0 to 300 K by assigning velocities every 0.1 ps from the Maxwellian distribution, at temperatures incremented by 50 K at each reassignment. Following this initial heating procedure, it was then equilibrated for 2 ps so as to relax itself at the same temperature. The trajectories were then continued for a subsequent period of simulation for 40 ps. Six structures were selected from this RMD-simulated conformational space based on the small values of NOE energies (less than 25 kcal/mol) and on fewer violations of distance constraints. The structures were finally subjected to 200 steps of constrained energy minimization in order to attain the conformational energy minima.

Discussion

Structure in Solution

An analysis of six selected structures indicates that enopeptin A has a highly ordered conformation

Table 3. Co-ordinates of heavy atoms obtained from one of the RMD structures of enopeptin A.

Atom[a]	x	y	z	Atom[a]	x	y	z
N(46)	−6.677	2.363	−0.086	C(21)	−7.523	4.613	7.503
C(2)	−7.947	2.403	0.643	N(59)	−8.840	3.989	7.491
C(3)	−8.975	1.950	−0.402	C(29)	−9.773	4.328	6.581
C(4)	−8.182	1.049	−1.356	C(30)	−11.073	3.620	6.574
C(5)	−6.772	1.651	−1.361	C(31)	−11.353	2.571	7.375
C(47)	−8.810	0.922	−2.748	C(32)	−12.629	1.839	7.420
C(6)	−5.554	2.980	0.382	C(33)	−13.782	2.221	6.837
C(7)	−4.311	2.922	−0.497	C(34)	−15.009	1.415	6.912
N(48)	−3.613	4.142	−0.182	C(35)	−16.194	1.761	6.375
C(9)	−2.755	4.744	−1.009	C(36)	−17.378	0.894	6.453
C(10)	−2.167	6.056	−0.459	C(37)	−18.585	1.185	5.930
N(49)	−2.591	6.375	0.923	C(38)	−19.745	0.282	5.993
C(12)	−2.159	5.578	1.952	C(39)	−19.798	−0.840	6.739
C(13)	−2.608	5.892	3.408	C(40)	−20.942	−1.771	6.728
C(14)	−1.591	5.278	4.383	N(60)	−21.981	−1.540	5.910
C(15)	−2.067	3.837	4.593	C(42)	−23.192	−2.364	5.756
C(16)	−3.585	3.894	4.415	C(41)	−24.348	−1.726	5.148
N(50)	−3.840	5.186	3.771	C(45)	−25.496	−2.714	5.044
C(17)	−5.072	5.749	3.610	C(44)	−24.874	−3.989	5.654
C(18)	−6.299	4.869	3.912	C(43)	−23.459	−3.644	6.052
C(19)	−7.457	5.153	2.936	O(61)	−24.357	−0.596	4.762
O(51)	−7.999	3.901	2.504	O(62)	−20.819	−2.713	7.497
C(1)	−8.266	3.792	1.219	O(63)	−22.610	−4.545	6.620
O(52)	−8.660	4.716	0.578	O(64)	−9.622	5.210	5.747
O(53)	−5.484	3.597	1.439	C(22)	−7.586	6.124	7.802
O(54)	−2.466	4.325	−2.119	O(65)	−6.243	3.110	6.131
O(55)	−1.444	4.608	1.746	C(23)	−8.417	6.428	9.022
O(56)	−5.225	6.909	3.250	C(24)	−9.705	6.940	8.888
C(11)	−0.646	6.106	−0.667	C(25)	−10.476	7.221	10.009
C(57)	−3.522	7.498	1.081	C(26)	−9.965	6.991	11.279
C(8)	−3.425	1.738	−0.111	C(27)	−8.682	6.480	11.422
N(58)	−6.776	5.133	5.259	C(28)	−7.912	6.202	10.299
C(20)	−6.769	4.209	6.223				

[a] The numbers of the heavy atom positions given in the parentheses correspond to Fig. 1.

for its cyclic moiety compared to its linear chain. This region is so well ordered due to the presence of a large number of sequential NOEs defining the fold of the peptide backbone and also due to the transannular NOEs in the cyclic part. Table 3 lists the coordinates of the heavy atoms obtained from one of the RMD structures. The good non-bonded contacts in all structures are indicated by the negative values (an average value = −15.85 kcal/mol) of the Lennard-Jones van der Waals energy. The agreement noted among the selected structures reveals the similarities of the solution conformers. Hence, they were superimposed for the best fit of the backbone atoms of the cyclic residues as shown in Fig. 4(a). From this figure it is seen that the aliphatic chain segment is disordered compared to the cyclic moiety. Fig. 4(b) shows the stereoview of the best fitted superposition of the backbone atoms in the cyclic moiety of the six selected structures of enopeptin A. This figure clearly reveals the convergence of the overall fold of the cyclic moiety and shows that the NMR-derived constraints tightly define the backbone conformation of the same. The goodness of the superposition can be emphasized by comparing the energy terms including NOE energies for all the six structures. Table 4 lists all the energy terms, such as bond length, bond angle, dihedral angle, improper torsion, L-J van der Waals, electrostatic, NOE and total energies. The energy values for all structures are in a close range. The total energy varies between −108.89 and −110.23 kcal/mol and the NOE energy ranges from 21.36 to 22.60 kcal/mole. The narrow range of variation in the energy terms and negative value of the total energy indicate that the RMD structures represent reasonable solution structures based on the experimental NOE constraints.

Fig. 4.

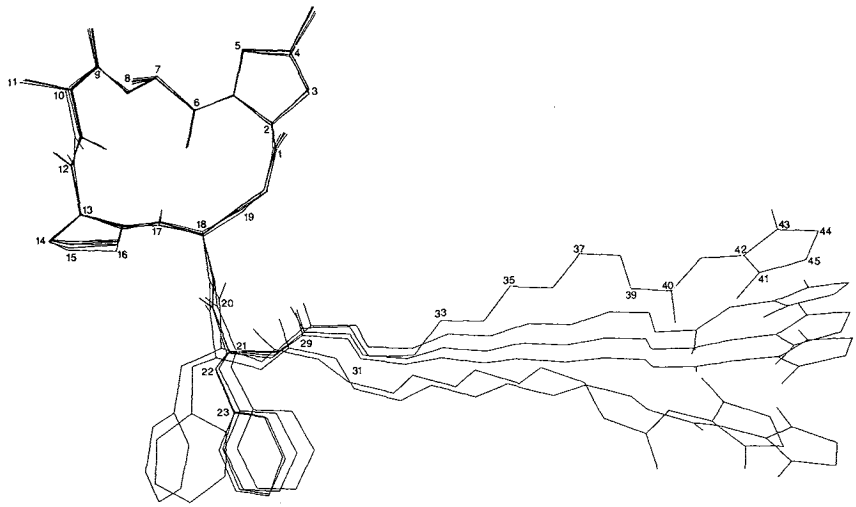

(a) Superposition of six enopeptin A structures obtained from RMD calculations.
Each member of the family of structures has been superimposed for the best fit of the backbone atoms of their cyclic moiety.

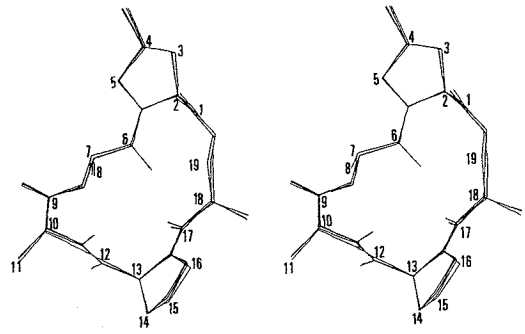

(b) Stereoview of the six RMD superposed structures showing the cyclic moiety alone.

Table 4. Energy values for the six selected RMD structures of enopeptin A.

Energy terms	RMD structures (kcal/mol)					
	1	2	3	4	5	6
Bond	1.67	1.81	1.76	1.77	1.62	1.65
Angle	35.67	37.48	38.52	37.96	37.23	37.07
Dihedral angle	40.99	38.74	38.35	38.84	37.83	40.10
Improper	0.84	0.71	0.65	0.62	0.58	0.52
Van der Walls	−15.67	−16.41	−15.59	−15.97	−15.67	−15.80
Electrostatic	−194.99	−193.38	−194.78	−194.10	−193.82	−195.13
NOE constraints	22.60	21.69	21.70	21.86	22.06	21.36
Total	−108.89	−109.37	−109.39	−109.02	−110.17	−110.23

The violations of distance constraints imposed by the NOE data also support the convergence of the solution structures and they are listed in Table 5. It includes the average values of the sum of violations of upper distance constraints imposed by NOE data (V_{ave}), the number of violations greater than 0.5 Å (V_n), and the maximum value of violations (V_{max}). This table reveals that the experimental NOE constraints have been strictly followed in all structures. As there are more NOE constraints in the cyclic moiety, a single family of converged conformations was observed for this segment.

Table 5. Violations of NOE distance constraints.

RMD structures	V_{ave} (Å)	V_{max} (Å)	V_n
1	0.35	0.72	5
2	0.31	0.66	5
3	0.27	0.77	4
4	0.38	0.70	4
5	0.36	0.99	4
6	0.38	0.73	5

The degree of closeness of the converged structures is obtained from the pairwise atomic root mean square deviation (RMSD) values (computed both for backbone and heavy atoms) of the cyclic moiety and the overall molecule, respectively (Table 6). The values indicated in the upper-right triangular matrix correspond to the backbone atoms of the cyclic moiety whereas those given in the lower-left correspond to the heavy atoms of the same. The corresponding data for the overall molecule are given in the parentheses. Thus, the RMSD values of the heavy atoms among the selected structures vary from 0.22 to 0.39 Å for the cyclic residues and from 0.17 to 1.9 Å for the whole molecule. The smaller values noted for the cyclic segment indicate its convergence. The higher values noted for the whole molecule imply the irregular conformation of the aliphatic chain segment.

Further evidence for the convergence of the calculated structures in the cyclic region is seen from the similarities of the dihedral angles (ϕ, ψ) in the selected structures. These data are presented in Table 7. The aliphatic segment of the molecule is the ill defined portion of the calculated structures, probably indicating that it is conformationally more flexible than the rest of the molecule. The narrow range of (ϕ, ψ) values for the cyclic moiety is clearly revealed in Table 7. Further the dihedral angles ϕ obtained from RMD calculations are comparable with those obtained from the NMR coupling constants (for Ala, Ser & Phe), duly confirming the results of RMD calculation. The flexibility in the conformation of the olefinic atoms is revealed from an analysis of the average atomic RMSD values computed from the six structures with respect to their mean. An analysis of these values indicates that the values for the olefinic atoms are greater than those for the cyclic portion, thus implying a flexible conformation for the aliphatic chain segment.

Thus an analysis of the solution conformation indicates that the molecule is oriented in such a way that most of the carbonyl oxygens of the cyclic moiety have an easy access to the molecular cavity. Regarding the conformation of the side chain orientations, the hydrophobic side chains of the cyclic amino acids (core region) protrude outwards. The latter may provide possibility for hydrophobic clustering with membrane systems. Thus, the calculated structure in solution enables interpretation of structure-activity studies in terms of the conformational features of the molecule.

In summary, according to conformational aspects of enopeptin A from NMR measurements, six

Table 6. The pairwise root-mean-square deviation values among the six selected RMD structures of enopeptin A[a].

RMD structures	1	2	3	4	5	6
				(backbone atoms)		
1	—	0.14	0.14	0.11	0.12	0.07
		(0.64)	(0.72)	(0.84)	(1.16)	(1.47)
2	0.25	—	0.03	0.06	0.10	0.14
	(0.71)		(0.17)	(0.29)	(0.78)	(1.24)
3	0.24	0.02	—	0.10	0.14	0.02
	(0.80)	(0.23)		(0.13)	(0.64)	(1.14)
4	0.20	0.06	0.05	—	0.03	0.03
	(0.93)	(0.35)	(0.17)		(0.55)	(1.09)
5	0.21	0.09	0.10	0.07	—	0.08
	(1.39)	(0.99)	(0.83)	(0.73)		(0.69)
6	0.15	0.15	0.14	0.11	0.13	—
	(1.91)	(1.74)	(1.62)	(1.56)	(1.06)	
			(heavy atoms)			

[a] The non-bracketed values refer to the cyclic moiety and the bracketed values correspond to the overall molecule.

Table 7. The backbone dihedral angles observed in the RMD structures for the cyclic fragment of enopeptin A.

Residues		RMD structures					
		1	2	3	4	5	6
Phe	ϕ	−64.14	−66.17	−66.70	−66.18	−63.21	−63.97
	ψ	86.14	100.10	92.58	93.20	90.63	81.87
Ser	ϕ	−114.20	−116.20	−81.71	−109.80	−116.80	−134.10
	ψ	84.87	97.29	95.99	93.12	91.12	80.01
Pro	ϕ	−83.97	−92.44	−90.87	−88.85	−90.08	−86.69
	ψ	112.50	91.10	91.82	95.50	95.33	98.37
MeAla	ϕ	60.67	67.48	67.57	66.85	67.45	68.98
	ψ	4.30	3.74	4.07	4.08	3.38	5.34
Ala	ϕ	−170.40	−155.30	−156.10	−159.50	−161.00	−166.20
	ψ	153.50	150.00	150.40	150.00	147.10	154.50
MePro	ϕ	44.28	42.68	40.88	40.88	44.18	44.33

structures derived from the RMD technique represent the conformations of enopeptin A in DMSO solution compatible with all experimental data. The backbone conformations of these structures indicate that enopeptin A possesses a stable conformation in solution. It is also implied that the residues in its core region adopt a highly ordered compact conformation with its cavity being surrounded by the carbonyl oxygens. The exact orientation of the molecule for its biological activity may be determined at least in part by the topology of the side chain hydrophobic residues and the cavity at the center of the cyclic moiety.

Acknowledgments

We thank the National Science Council (NSC 82-0208-M007-007) of the Republic of China for support.

References

1) OSADA, H.; T. YANO, H. KOSHINO & K. ISONO: Enopeptin A, a novel depsipeptide antibiotic with anti-bacteriophage activity. J. Antibiotics 44: 1463~1466, 1991
2) KOSHINO, H.; H. OSADA, T. YANO, J. UZAWA & K. ISONO: The structure of enopeptins A and B, novel depsipeptide antibiotics. Tetrahedron Lett. 32: 7707~7710, 1991

3) MOLONEY, G. P.; D. J. CRAIK & M. N. ISKANDER: ^{1}H and ^{13}C studies of aminoglycoside antibiotics. Magn. Res. Chem. 31: 1077~1084, 1993
4) BALAKRISHNAN, A. R. & K. R. K. EASWARAN: Conformation of polyene antibiotic, Filipin III: CD and ^{1}H NMR studies. J. Biomolec. Str. Dyn. 11: 417~428, 1993
5) SOWINSKI, P.; J. PAWALAK, E. BOROWSKI & P. GARIBOLDI: ^{1}H NMR model studies of Amphotericin B: Comparison of X-ray and NMR stereochemical data. Magn. Reson. Chem. 30: 275~279, 1992
6) LANCELIN, J. M. & J. M. BEAU: Stereochemistry of pimaricin. J. Am. Chem. Soc. 112: 4060~4061, 1990
7) SOWINSKI, P.; P. GARIBOLDI, A. CZERWINSKI & E. BOROWSKI: The structure of vacidin A, an aromatic heptaene macrolide antibiotic. J. Antibiotics, 32: 1631~1638, 1989
8) LANCELIN, J. M.; F. PAQUET & J. M. Beau: Stereochemical studies on the polyene macrolide Nystatin A_1: The hydroxyl groups on the C-1~C-10 fragment are all-syn. Tetrahedron Lett. 29: 2827~2830, 1988
9) BONZLI, P. & J. T. GERIG: Conformational analysis of the mushroom toxin phallacidin by ^{1}H NMR spectroscopy and restrained molecular dynamics. J. Am. Chem. Soc. 112: 3719~3726, 1990
10) RIZO, J.; S. C. KOERBER, R. J. BIENSTOCK, J. RIVIER, L. M. GIERASCH & A. T. HAGLER: Conformational analysis of a highly potent, constrained gonadotropin-releasing hormone antagonist. 1. Nuclear magnetic resonance. J. Am. Chem. Soc. 114: 2852~2859, 1992
11) KOPPLE, K. D.; P. W. BAURES, J. W. BEAN, C. A. D'AMBROSIO, J. L. HUGES, C. E. PEISHOFF & D. S. EGGLESTON: Conformations of Arg-Gly-Asp containing heterodetic cyclic peptides: solution and crystal studies: J. Am. Chem. Soc. 114: 9615~9623, 1992
12) WON, H.; K. D. OLSON, D. R. HARE, R. S. WOLFE, C. KRATKY & M. F. SUMMERS: Structural modelling of small molecules by NMR: solution state structure of 12,13-diepimeric coenzyme F430 and comparison with the X-ray structure of the pentamethyl ester derivative. J. Am. Chem. Soc. 114: 6880~6892, 1992
13) CLORE, G. M.; A. M. GRONENBORN, A. T. BRUNGER & M. KARPLUS: Solution conformation of heptapeptide comprising the DNA binding helix F of the cyclic AMP receptor protein of Escherichia coli. Combined use of ^{1}H nuclear magnetic resonance and restrained molecular dynamics. J. Mol. Biol. 186: 435~455, 1985
14) BAX, A. & R. FREEMAN: Investigation of complex networks of spin-spin coupling by two-dimensional NMR. J. Magn. Reson. 44: 542~561, 1981
15) DAVIS, D. G. & A. BAX: Assignment of complex proton NMR spectra *via* two-dimensional homonuclear Hartmann-Hahn spectroscopy. J. Am. Chem. Soc. 105: 2821~2823, 1985
16) BAX, A. & D. G. DAVIS: MLEV-17 based two-dimensional homonuclear magnetization transfer spectroscopy. J. Magn. Reson. 65: 335~360, 1985
17) BOTHNER-BY, A.; R. L. STEPHENS, J. T. LEE, C. D. WARREN & R. W. Jeanloz: Structure determination of a tetrasaccharide: transient nuclear Overhauser effects in the rotating frame. J. Am. Chem. Soc. 106: 811~813, 1984
18) KESSLER, H.; C. GRIESINGER, R. KERSSEBAUM, K. WAGNER & R. R. ERNST: Separation of cross-relaxation and *J* cross-peaks in 2D rotating-frame NMR spectroscopy. J. Am. Chem. Soc. 109: 607~609, 1987
19) BALEJA, J. D.; J. MOULT & B. D. SYKES: Distance measurement and structure refinement with NOE data. J. Magn. Reson. 87: 375~384, 1990
20) BALEJA, J. D.; R. T. PON & B. D. SYKES: Solution structure of phage half-operator DNA by use of NMR, restrained molecular dynamics and NOE based refinement. Biochemistry 29: 4828~4839, 1990
21) BYSTROV, V. F.: Spin-spin coupling and the conformational states of peptide systems. Prog. NMR Spectrosc. 10: 41~81, 1976
22) BROOKS, B. R.; R. E. BRUCCOLERI, B. D. OLAFSON, D. J. STATES, S. SWAMINATHAN & M. KARPLUS: CHARMm: a program for macromolecular energy minimization and dynamics calculations. J. Comput. Chem. 4: 187~217, 1983
23) WÜTHRICH, K.: NMR of Proteins and Nucleic Acids, John Wiley and Sons, New York 1986
24) WÜTHRICH, K.; M. BILLETER & W. BRAUN: Pseudostructures for the 20 common amino acids for use in studies of protein conformations by measurements of intramolecular proton-proton distance constraints with nuclear magnetic resonance. J. Mol. Biol. 169: 949~961, 1983